



AUTHOR(S):

TITLE:

YEAR:

Publisher citation:

OpenAIR citation:

Publisher copyright statement:

This is the _____ version of an article originally published by _____
in _____
(ISSN _____; eISSN _____).

OpenAIR takedown statement:

Section 6 of the "Repository policy for OpenAIR @ RGU" (available from <http://www.rgu.ac.uk/staff-and-current-students/library/library-policies/repository-policies>) provides guidance on the criteria under which RGU will consider withdrawing material from OpenAIR. If you believe that this item is subject to any of these criteria, or for any other reason should not be held on OpenAIR, then please contact openair-help@rgu.ac.uk with the details of the item and the nature of your complaint.

This publication is distributed under a CC _____ license.

Effect of electron beam irradiation on the structural and optical properties of Cu doped In₂O₃ films prepared by RF magnetron sputtering

R. Reshmi Krishnan¹, Ganesh Sanjeev², Radhakrishna Prabhu³ and V.P. Mahadevan Pillai¹

¹Department of Optoelectronics, University of Kerala, Kariavattom,
Thiruvananthapuram– 695581, Kerala, India

²Department of Physics, Mangalore University, Mangalagangotri, Karnataka, India

³School of Engineering, Robert Gordon University, Aberdeen, UK

E-mail: vpmpillai9@gmail.com

Abstract. Undoped and Cu doped In₂O₃ films are prepared by radio frequency magnetron sputtering technique. The effects of Cu doping and high energy electron beam irradiation on the structural and optical properties of as-prepared films are investigated using techniques such as X-ray diffraction, X-ray photoelectron spectroscopy (XPS), lateral scanning electron microscopic image analysis, energy dispersive X-ray (EDX) spectroscopy, micro-Raman and UV-visible spectroscopy. Moderate doping of Cu in In₂O₃ enhances the intensity of (222) peak indicating the alignment of crystalline grains along <111>. Electron beam irradiation promotes the orientation of crystalline grains along <111> in undoped and moderate Cu doped films. EDX spectroscopic analysis and XPS analysis reveal the incorporation of Cu²⁺ ions in the lattice. Transmittance of Cu doped films decreases with e-beam irradiation. A systematic reduction of bandgap energy with increase in Cu doping concentration can be seen in unirradiated and electron beam irradiated films.

Introduction

In₂O₃ with direct band gap energy of 3.55-3.75 eV [1] has attracted much interest as an important functional oxide semiconductor in both fundamental research and practical studies [2]. It finds applications as transparent windows in liquid crystal displays [3], solar cells [4], electrochromic devices [5], optoelectronic devices [6], gas sensors [7] etc., owing to its electrical conductivity and high optical transparency in the visible region [8]. The optical and electrical properties of semiconductors depend on the inclusion of dopants in the host material as well as on its structural parameters such as bond length, crystallite size, lattice constants, stress-strain mechanism etc. [9]. Copper oxide (CuO) is a p-type semiconductor possessing an indirect band gap energy in the range 1.2-1.9 eV [10,11]. CuO-based materials have a variety of applications in optoelectronics, catalysis etc. owing to their distinct properties [10]. Wen et al. prepared In₂O₃, In₂O₃:SnO₂ and Cu doped In₂O₃, In₂O₃:SnO₂ ceramics, investigated the transport properties of the ceramics and analysed the relation between carrier concentration, mobility and density. They observed a decrease in the absorbance in In₂O₃ ceramics with increase in Cu doping concentration whereas in In₂O₃:SnO₂ ceramics, they observed an increase in the absorbance with increase in Cu doping concentration [12]. Copper indium oxide films prepared by Singh et al. by reactive RF magnetron sputtering technique at different substrate temperatures namely 300 and 400 °C showed two values of band gap energy (i.e. 3.3 and 4.3 eV) [13]. Kaleemulla et al. studied the influence of annealing temperature on the morphological, structural and optical properties of Cu doped films synthesized by the method of flash evaporation. An enhancement in the transmittance

of the films with increase in annealing temperature was reported [14]. Cu doped In_2O_3 films with varying Cu concentration were synthesized using perfume atomizer technique by Deepa et al. [11,15]. They observed intense UV emission and low values for electrical resistivity for the films. In_2O_3 : Cu films were synthesized using electron beam evaporation technique by Krishna et al. and they analysed the effect of Cu concentration on the structural and magnetic properties of the In_2O_3 films. An enhancement in the concentration of oxygen vacancies and strength of ferromagnetic behaviour with increase in Cu concentration was reported. They related the ferromagnetic property to the oxygen defect mediated ferromagnetic exchange between two Cu^+ ions [16].

Irradiating materials with high energy electron beam can modify its microstructure, crystal structure and change the physical properties [17-19] and hence affects the optical and electrical properties. Intrinsic stress in the vacuum deposited amorphous films can be either reduced or enhanced with irradiation, thereby modifying its structural and optical properties [20]. Fast electrons (with kinetic energies > 10 keV), being charged particles, interact strongly with both atomic nuclei and electrons in a Coulombic manner [21]. Most of the energy losses at high energy electron bombardment are caused by electron-electron collisions, rather than the electron-nucleus collisions. Electron-electron collisions lead to film heating, which results in radiation annealing and relaxation of the lattice [22]. Thus, interaction of electron with materials can be the key factor for induced modification of properties of materials. In the present work, the effect of Cu doping on the structural and optical properties of In_2O_3 films prepared by RF magnetron sputtering are investigated. The influence of electron beam irradiation on the structural and optical properties of undoped and Cu doped In_2O_3 films is also analyzed.

Experimental details

Undoped and Cu-doped In_2O_3 films were prepared by RF magnetron sputtering technique. CuO powder with different mole percentage (0, 1, 2, 4, 6 and 10 mole %) were added to In_2O_3 powder (Sigma Aldrich 99.99% purity) and grounded well. This powder mixture was pressed and used as the targets for sputtering. The deposition chamber was first evacuated to a base pressure of 3×10^{-6} mbar and pure argon gas was admitted to the chamber (Ar pressure-0.015 mbar). Deposition of the films was done on quartz substrates (substrate- target distance-5cm), for a duration of 40 minutes using an RF power of 120 W. The as-deposited films with different Cu doping concentrations (viz., 0, 1, 2, 4, 6 and 10 mole %) are designated as ICu0, ICu1, ICu2, ICu4, ICu6 and ICu10 respectively. The films were irradiated with electron beam using 8 MeV Microtron facility at Mangalore University, Mangalagangothri, India. Samples (1 cm^2 in size) sealed in transparent thin polythene sheets were exposed to e- beam at 30 cm from the beam exit port at a pulse repetition rate of 50 Hz. The electron doses delivered to the samples were monitored using a current integrator calibrated with appropriate radiation dosimeters. The samples were irradiated for 5kGy doses at a dose rate of around 200 Gy per minute. The dose delivered has a uniform distribution of 8 cm x 8 cm area. The irradiated samples with respective Cu doping concentrations are coded as RICu0, RICu1, RICu2, RICu4, RICu6 and RICu10 respectively.

Structural properties of unirradiated and irradiated films were investigated by X-ray diffraction (Bruker AXS D8 Advance) measurements employing $\text{CuK}\alpha 1$ radiation with a wavelength of 1.5406 \AA in the 2θ range 20° - 70° . Micro-Raman spectra of the films were recorded using Labram HR-800 (Horiba JobinYvon) spectrometer with a spectral resolution $\sim 1 \text{ cm}^{-1}$ using an excitation radiation of 514.5 nm from an argon ion laser. Transmittance spectra of the films were recorded using a UV-Visible (JASCO, V-550) double beam spectrophotometer. The thickness of the films was estimated by a Nova Nano SEM 450 (FEI) field emission scanning electron microscope (FESEM) using lateral FESEM images. The elemental analysis of the films was carried out using electron energy dispersive X-ray spectrometer (EDS-Quantax 200, Germany) attached with FESEM. X-ray photoelectron spectra (XPS) were recorded with XPS spectrometer (Omicron Technology) with monochromatic $\text{Al K}\alpha$ (1486.7 eV) X-ray source.

Results and discussions

Figure 1(a) shows XRD patterns of unirradiated In_2O_3 films with different Cu doping concentrations. XRD patterns reveal polycrystalline nature for all the unirradiated films. XRD pattern of ICu_0 film presents an intense peak at 2θ value 30.60° and a weak peak at 2θ value 21.47° corresponding to (222) and (211) lattice reflection planes of cubic bixbyite crystalline phase of In_2O_3 respectively [JCPDS Card No. 71-2195]. The broad hump like structure in the 2θ range 15° - 30° observed in the XRD pattern for ICu_0 film indicates that the film is not fully crystalline in nature. XRD patterns of Cu doped In_2O_3 films also reveal the formation of cubic bixbyite phase in them. In ICu_1 film, the intensity of (222) peak increases by 3.86 times compared to that of ICu_0 film and a peak corresponding to (440) lattice reflection plane of cubic bixbyite phase also appeared.

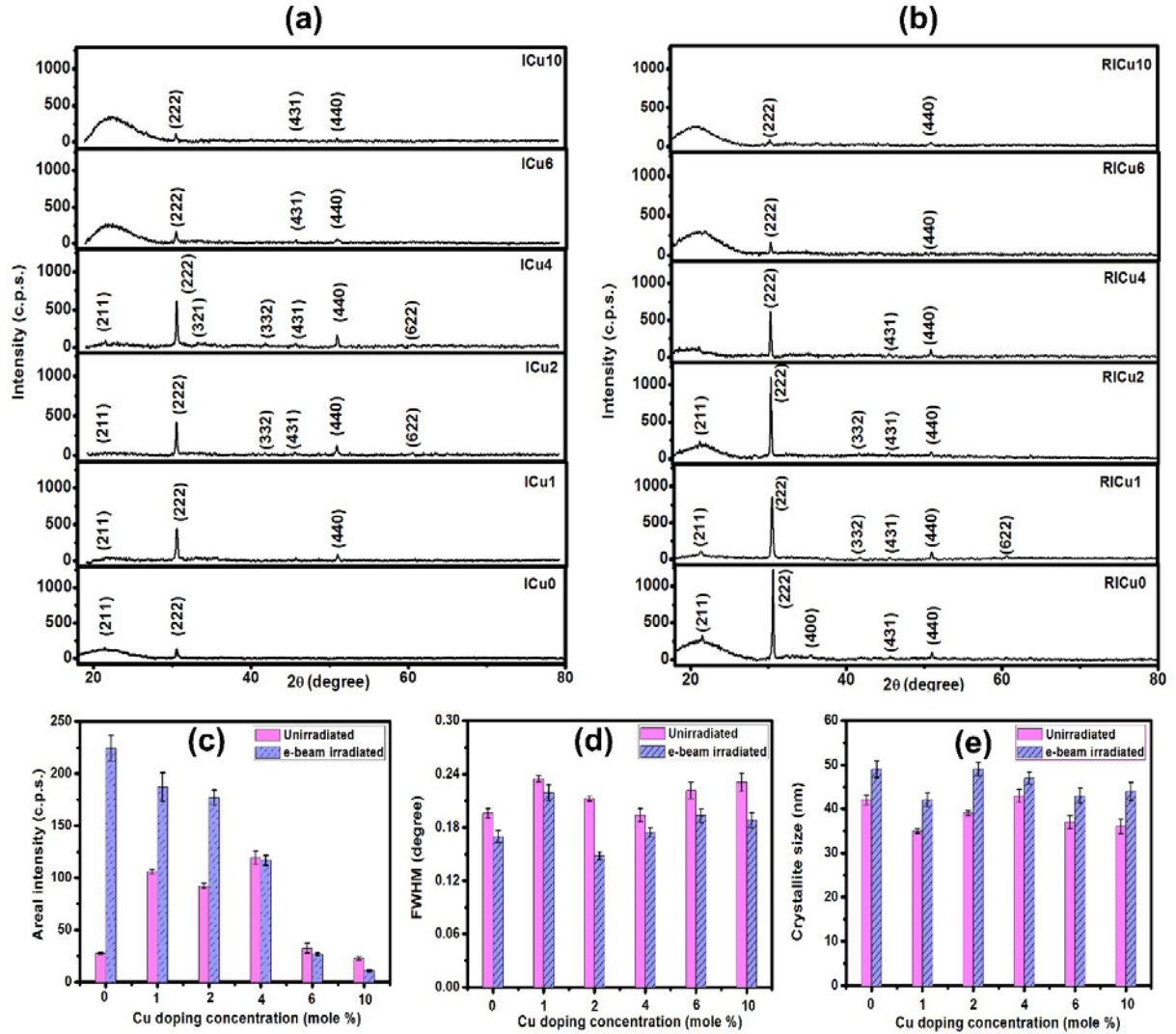


Fig. 1. XRD patterns of undoped and Cu doped In_2O_3 films: (a) unirradiated and (b) electron beam irradiated. Variation of: (c) areal intensity of (222) peak, (d) FWHM of (222) peak and (e) crystallite size of unirradiated and irradiated Cu doped In_2O_3 films with doping concentration. The error bars are shown in the figure.

The XRD patterns of ICu2 and ICu4 films show three additional weak peaks corresponding to lattice reflection planes (332), (431) and (622) respectively of cubic bixbyite In_2O_3 phase. The intensity of the (222) peak in ICu2 and ICu4 films are respectively 3.37 and 4.34 times that of ICu0 film (Fig. 1(a) and 1(c)). The hump like structure observed in the XRD pattern of ICu0 film almost disappeared in the XRD patterns of ICu1, ICu2 and ICu4 films. In the XRD patterns of ICu6 and ICu10 films, two peaks corresponding to lattice reflection planes (222) and (440) are only visible, that too with less intensity. Also, the hump like structure reappears in the XRD patterns of these two films. In all the unirradiated films, (222) peak shows the highest intensity. For cubic bixbyite phase, (222) is the plane with high atomic density and lower surface energy [23]. Among the unirradiated films investigated, ICu4 film

possesses the lowest value of full width at half maximum (FWHM) for (222) peak. The highest intensity and the lowest value of FWHM for (222) peak for ICu4 film suggests its superior crystalline quality. Moderate doping of Cu in In_2O_3 lattice seems to promote the preferred orientation of crystal growth along (222) plane.

XRD patterns of e-beam irradiated films are shown in Fig. 1(b). In the XRD pattern of the e-beam irradiated undoped film (RICu0), the intensity of the (222) peak is about 8.18 times that of the intensity observed for ICu0 film. FWHM of the (222) peak in RICu0 is 0.1697° whereas in ICu0 film, it is 0.1957° . These observations suggest that the crystallinity of the undoped film has enhanced considerably on irradiating with e-beam. On irradiation of the film, energy can be transferred from the e-beam to the crystal lattice. Microscopic arrangement of nanocrystals or rearrangement of atoms may also take place in the film due to irradiation [24]. High temperature can increase the atomic mobility which may increase the ability of atoms to find the most energetically favoured sites. This can result in better crystalline quality of the films [25]. In films with 1 and 2 mole % Cu doping also, the (222) peak shows enhancement in intensity on e-beam irradiation. The intensity of this peak in these films on e-beam irradiation is respectively 1.77 and 1.92 times that of their unirradiated counterparts (Fig 1(c)). No significant change in the intensity of (222) peak is observed on e-beam irradiation in films with higher Cu doping concentration. Some additional peaks with less intensity can be seen in the XRD patterns of RICu0 film and irradiated films with moderate Cu doping concentration. FWHM values of (222) peak in all the irradiated samples are lower than that in unirradiated films (Fig. 1(d)). Among the irradiated films, RICu4 film shows lowest value of FWHM (0.1481°) and RICu0 film shows the highest intensity for (222) peak.

The texture coefficient (TC) is a measure of preferred orientation of the films. TC can be calculated from the measured intensity of the (hkl) plane [$I(hkl)$] and the standard intensity of the (hkl) plane [$I_0(hkl)$] taken from the JCPDS data card by the following relation [26,27]:

$$TC(hkl) = \frac{I(hkl)/I_0(hkl)}{N^{-1} \sum I(hkl)/I_0(hkl)} \quad (1)$$

TC for (222) and (440) planes are calculated for unirradiated and irradiated films (Table I). The value of $TC > 0$ but less than one suggests lack of grains in a particular (hkl) direction. $TC(hkl) = 1$ represents films with randomly oriented crystallites indicating the lack of preferred orientation while higher values of $TC(hkl)$ [$TC > 1$] indicate the abundance of grains oriented in a given (hkl) direction indicating the preferred orientation [26, 28]. Among the unirradiated samples, ICu0, ICu6 and ICu10 possess values $TC=1$, indicating the lack of preferred orientation in them. ICu1, ICu2 and ICu4 films possess TC value >1 for (222) plane indicating that $\langle 111 \rangle$ can be the preferred direction of crystalline growth in them. All the irradiated samples except RICu6 and RICu10 films show preferred direction of crystalline growth along $\langle 111 \rangle$.

In the unirradiated films, moderate Cu doping enhances the intensity of the (222) peak. The undoped and moderately Cu doped films show appreciable enhancement in intensity of the (222) peak on e-beam irradiation. The

enhancement in the intensity along a particular plane can be due to the orientation of crystallites along that plane, enhancement of the crystallinity of the material or due to the film thickness. The thickness of the films is estimated using lateral FESEM images (Fig. 2 (a)) and the observed values are listed in Table I. The values of thickness lie in the range 198-230 nm. The thickness of ICu6 and ICu10 films is found to be higher than that of ICu0 film but the intensity of the (222) peak in these films doesn't change much. Average size of the crystallites is calculated using Scherrer formula [29] for both unirradiated and e-beam irradiated films. In the unirradiated films, average size of crystallites ranges from 35 nm to 47 nm whereas in irradiated films, it is in the range 42-49 nm (Fig. 1(e)). The average size of the crystallites in all the films increases by e-beam irradiation.

The lattice strain in the unirradiated and e-beam irradiated Cu doped In_2O_3 films is calculated using the relation [29]:

$$T \tan \theta = \frac{\lambda}{D \cos \theta} - \beta \quad (2)$$

where T is the lattice strain, λ is the wavelength of X-rays used, θ is the Bragg angle, D is the crystallite size, and β is the FWHM of intense (222) peak. Cu doping in In_2O_3 lattice does not affect the lattice strain significantly (Table I). A slight reduction in the value of lattice strain can be seen for e-beam irradiated films. The observed reduction in the lattice strain in the films can be due to the thermal effect as a result of e-beam irradiation. The calculated values of lattice constant for the films are given in Table I.

A shift of the XRD peaks from the corresponding stress-free data of the bulk material suggests the existence of stress in the films which depends on the material and the synthesizing conditions [30,31]. Several factors which result in the development of stress include lattice mismatch, difference in thermal expansion coefficient between the film and the substrate, dynamic processes such as inter-diffusion, recrystallization, impurities, voids, dislocations, ionic size mismatch between the host and dopant ions etc. [32,33]. The (222) peak position of the unirradiated films are shifted towards higher 2θ angles compared to the In_2O_3 powder [JCPDS Card No. 71-2195] suggesting the presence of compressive stress in them. For the unirradiated films, even though we do not observe a monotonic shift of the (222) peak position with varying Cu concentration, all the films except ICu2 film show a shift of (222) peak towards higher diffraction angles. The ionic radius of Cu^{2+} ions (0.074 nm) [34] that of In^{3+} ions (0.080 nm) [35]. We can expect a slight shrinkage of lattice when Cu ions of lower ionic radius gets substituted for In ions of higher ionic radius. As a result, the peak may get shifted to higher angles. On e-beam irradiation, the intense (222) peak shows a shift towards lower 2θ values in undoped and doped films with Cu concentration up to 4 mole % whereas in films with higher doping concentration, (222) peak shows a shift to higher 2θ values on e-beam irradiation. A shift of the XRD peaks towards lower angles is an indication of tensile stress [31,36]. Hence, it is found that the compressive stress of the undoped and moderately Cu doped In_2O_3 films changes to tensile stress on e-beam irradiation whereas the higher doped films retain its compressive stress. This can be attributed to the annihilation of dislocations/defects as well as due to the growth of grains induced by e-beam irradiation [31].

Table I Structural and optical parameters of unirradiated and electron beam irradiated Cu doped In₂O₃ films deposited on quartz substrate by RF magnetron technique.

Cu doping concentration (mole %)	FWHM of (222) peak (°)		Texture coefficient of (222) plane		Texture coefficient of (440) plane		Lattice constant a (Å)		Lattice strain		Thickness of films (nm)	Bandgap (eV)	
	*U	#I	*U	#I	*U	#I	*U	#I	*U	#I		*U	#I
0	0.1957	0.1697	1	1.67	-	0.33	10.113 ±0.0129	10.116 ±0.0129	0.0014 ±0.00036	0.0012 ±0.00042	198	3.60 ±0.06	3.53 ±0.03
1	0.2348	0.2189	1.26	1.49	0.37	0.51	10.112 ±0.0129	10.125 ±0.0129	0.0017 ±0.00030	0.0016 ±0.00032	200	3.57 ±0.03	3.52 ±0.01
2	0.2125	0.1481	1.17	1.59	0.83	0.41	10.121 ±0.0129	10.122 ±0.0129	0.0015 ±0.00033	0.0011 ±0.00048	216	3.56 ±0.05	3.51 ±0.03
4	0.1934	0.1742	1.13	1.38	0.87	0.62	10.105 ±0.0128	10.112 ±0.0129	0.0014 ±0.00037	0.0012 ±0.00041	230	3.54 ±0.05	3.48 ±0.01
6	0.2216	0.1930	1	1	-	-	10.109 ±0.0128	10.103 ±0.0128	0.0016 ±0.00032	0.0014 ±0.00037	211	3.49 ±0.03	3.43 ±0.02
10	0.2308	0.1879	1	1	-	-	10.113 ±0.0129	10.105 ±0.0128	0.0016 ±0.00031	0.0013 ±0.00038	205	3.45 ±0.03	3.41 ±0.01

*U-unirradiated films, #I- electron beam irradiated films

Lattice constant of bulk In₂O₃-10.118 Å

The XRD analysis gives an indication of the substitution of Cu²⁺ ions in the sites of In³⁺ ions. To verify the incorporation of Cu ions, elemental analysis using EDX spectroscopy and XPS are carried out. EDX analysis (Fig. 2 (b) and 2 (c)) shows the incorporation of Cu in the film. Both the analysis show the incorporation of Cu in the films.

Metal oxide semiconductor films have imperfect surfaces even when impurities are absent. These imperfections can act as acceptors or donors [37]. The various defects present in semiconductor oxides include oxygen/metal vacancies, oxygen/metal interstitials etc. [38,39]. The presence of defects mainly the oxygen vacancies directly or indirectly determine the reactivity and surface chemistry of metal oxides [40]. Metal interstitials and oxygen vacancies can lead to oxygen deficient oxides relative to the stoichiometric composition [39]. In oxides, oxygen vacancies may be generated naturally [40]. Optimization of preparation conditions also play a significant role on the stoichiometry of the film. The oxygen vacancies may be present at the oxide surface or within the bulk [40] and their presence can control the electronic structure, optical, chemical, transport and magnetic characteristics of the material [40-42]. Oxygen vacancies can lead to shallow level defects or traps near the conduction band and can tune the band structure of materials [43]. The performance of the material in various applications can also be affected by the formation of defects/oxygen vacancies [41]. In the present study, the films are deposited under high vacuum conditions. This can result in the formation of non-stoichiometric films which are oxygen deficient. In the present case, XPS analysis suggest the formation of oxygen deficient films.

Gaussian fitting of the In 3d core level spectra show double peaks with a spin orbit splitting of 7.6 eV, corresponding to the characteristic In 3d_{3/2} and In 3d_{5/2} levels (Fig. 2 (d) and 2 (e)). This indicates the presence of In in +3 oxidation state in the films [44]. The O 1s XPS spectra on deconvolution (Fig. 2 (d) and 2 (e)) gives two peaks- O_I and O_{II}. The O_I peak ~ 529.45 eV in the films can be assigned to In-O bonding in In₂O₃ [45] and the O_{II} peak ~ 531.36 eV in the films is related to O²⁻ ions in the oxygen deficient region or to the surface adsorbed oxygen [46]. The core level spectra of Cu 2p region depicted in Fig. 2 (f) show very weak peaks of Cu²⁺ [47] which might be due to the low concentration of Cu in the doped films.

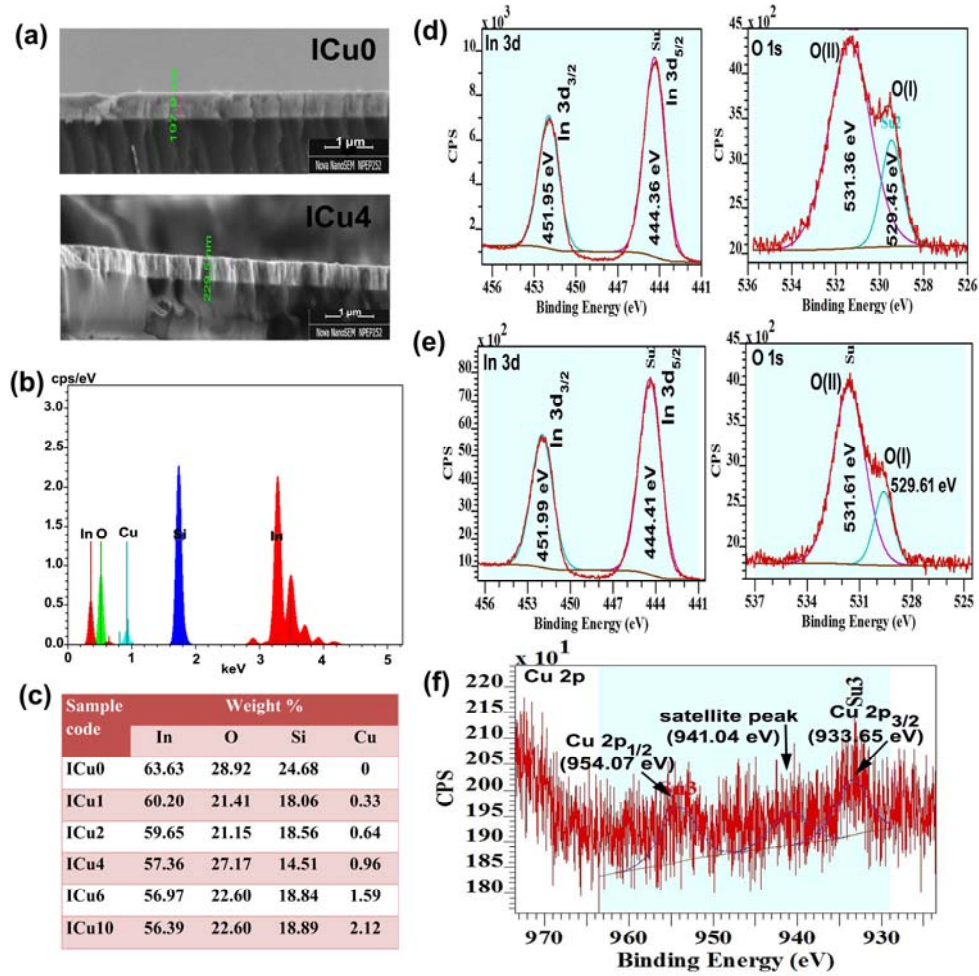


Fig. 2. (a) Typical cross-sectional FESEM images of unirradiated Cu doped In₂O₃ films showing the thickness of the films-ICu0 and ICu4, (b) EDX spectrum of 10 mole % unirradiated Cu doped In₂O₃ film, (c) table showing the composition of elements in unirradiated Cu doped In₂O₃ films, (d) In 3d and O 1s spectra of ICu0 film, (e) In 3d and O 1s spectra of ICu10 film and (f) Cu 2p spectrum of ICu10 film.

Micro-Raman spectra of typical films (undoped film and films with Cu doping concentrations 2 mole % and 10 mole %) which are unirradiated and irradiated with e-beam are shown in Figure 3(a)-3(f). In₂O₃ crystallises in cubic bixbyite structure with space group *Ia3* having 8 formula units per Bravais unit cell. Raman spectra of all the

films are characterized by a broad intense band extending from 200-550 cm^{-1} along with a number of medium intense to weak bands. Apart from slight intensity variation among the peaks, the spectral features remain almost same in all the films indicating that Cu incorporation do not affect the spectral behaviour of In_2O_3 film. On deconvolution, the broad spectral feature extending from 250-700 cm^{-1} yields 5 spectral components $\sim 365, 449, 495, 602$ and 625 cm^{-1} (shown in inset). Raman bands at 107, 117, 133 and 493 cm^{-1} have been reported for cubic bixbyite In_2O_3 [48,49]. Frost et al. observed additional bands at 186, 208 and 220 cm^{-1} in In_2O_3 powder [50]. Krishnan et al. have observed an additional band at 170 cm^{-1} in In_2O_3 powder [51].

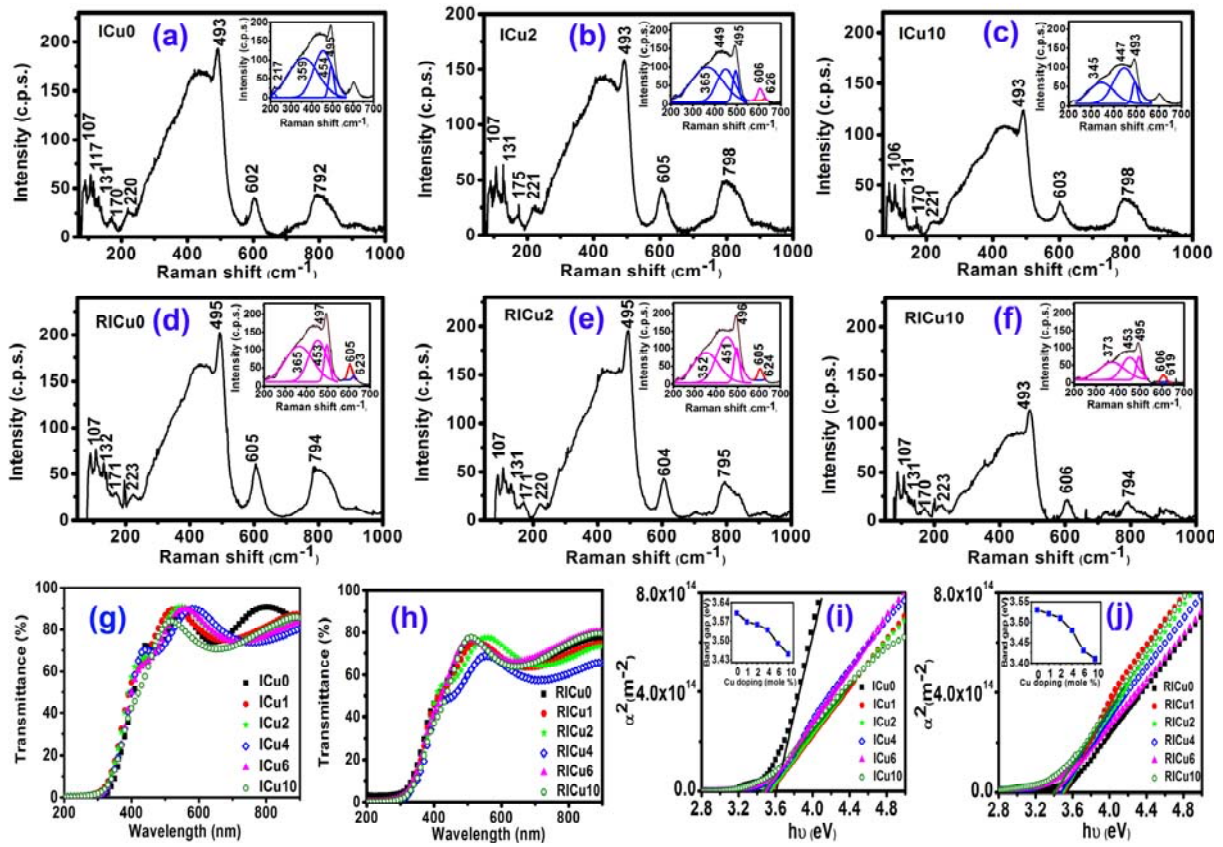


Fig. 3. (a)-(f) Micro-Raman spectra of typical unirradiated and irradiated Cu doped films: Deconvoluted spectra is shown as inset. Transmittance spectra of films: (g) unirradiated, (h) irradiated and α^2 vs $h\nu$ plots of films: (i) unirradiated, (j) irradiated. Variation of band gap energy with Cu doping concentration is shown as inset of (i) and (j).

The observation of Raman bands at 107, 117, 131, 170, 220 and 493 cm^{-1} confirms the presence of cubic bixbyite In_2O_3 phase in the films [48,49]. Low frequency mode observed at $\sim 107 \text{ cm}^{-1}$ can be ascribed to typical T_g mode of cubic In_2O_3 [52] and the band at $\sim 131 \text{ cm}^{-1}$ can be attributed to In-O vibration of InO_6 structural unit [53].

The mode at 220 cm^{-1} can be assigned to O-In-O bending modes [50]. Modes at ~ 493 and 626 cm^{-1} can be assigned to octahedral stretching vibrations of InO_6 structural unit [54]. Raman band $\sim 365\text{ cm}^{-1}$ can be attributed to stretching vibrations of In-O-In bridge and can be an indication of oxygen vacancies in the structure [53]. The bands ~ 602 and 807 cm^{-1} may be due to the spectral contribution from quartz substrate [55]. Electron beam irradiation does not significantly influence the spectral behaviour of In_2O_3 films.

Transmittance spectra of unirradiated and e-beam irradiated Cu doped In_2O_3 films are shown in Figure 3(g) and 3(h) respectively. ICu0 film presents an average transmittance of 80% in the 400 to 900 nm wavelength region. In the unirradiated films, a slight systematic reduction in transmittance with increase in Cu doping concentration (from 80% to 75%) can be seen. Irradiated films show lower values of transmittance compared to their unirradiated counterparts. The band gap values for unirradiated and e-beam irradiated films are estimated from the plots of α^2 versus $h\nu$ (Figure 3(i) and 3(j)) by extrapolating the linear portion of the curve and bandgap values are given in Table I [56]. Linear dependence of α^2 with $h\nu$ at higher photon energies in unirradiated and irradiated films indicates direct transition in them. ICu0 film possesses a band gap of 3.60 eV. Unirradiated Cu doped films show lower values of bandgap energies. Among the irradiated films, the undoped film shows the highest value of bandgap energy=3.53 eV. A systematic reduction of bandgap with increase in Cu doping concentration can be seen in both unirradiated and irradiated Cu doped films.

Conclusions

The structural and optical properties of In_2O_3 films with respect to Cu doping concentration and electron beam irradiation are investigated. XRD patterns of both unirradiated and e-beam irradiated films reveal the formation of cubic bixbyite phase of In_2O_3 . Moderate Cu doping promotes the orientation of grains along $\langle 111 \rangle$. On irradiating with the e-beam, undoped and moderate Cu doped films show enhancement in intensity of the (222) peak. Texture coefficient determination shows that irradiation promotes the alignment of crystallites along the $\langle 111 \rangle$ direction in undoped and moderately Cu-doped films. The stress in the undoped and moderate Cu doped films changes from compressive stress to tensile stress on e-beam irradiation. Average size of the crystallites in the irradiated films is found to be higher than that in their unirradiated counter parts. XPS and EDX analysis of the films suggest the incorporation of Cu in the films. XPS analysis suggests +3 oxidation state for In ions and +2 oxidation state for Cu ions. Micro-Raman analysis reveals the presence of characteristic bands of cubic bixbyite phase of In_2O_3 in the films. Electron beam irradiation does not significantly influence the spectral behaviour of In_2O_3 films. All the films show good average transmittance. Both unirradiated and irradiated Cu doped films possess lower bandgap values compared to undoped film.

References

- [1] A. Murali, A. Barve, V.J. Leppert and S.H. Risbud,; *Nano Lett*,1, 287 (2001).
- [2] H. Yang, S. Wang and Y. Yang,; *CrystEngComm*, 14, 1135 (2012).
- [3] Y. Shigesato, S. Thalaki and T. Haranoh,; *J. Appl.Phys*, 71, 3356 (1992).

- [4] Y. Sobajima, H. Muto, Y. Shinohara, C. Sada, A. Matsuda and H. Okamoto,; *Jpn. J. Appl. Phys*, 51, 10NB05-1 (2012).
- [5] C.G. Granqvist,; *Appl. Phys. A, Solids Surf*, 57, 19 (1993).
- [6] Hamberg and C.G. Granqvist,; *J. Appl. Phys*, 60, R123 (1986).
- [7] M. Kumar, B.R. Mehta, V.N. Singh, R. Chatterjee, S. Milikisiyants, K.V. Lakshmi and J.P. Singh,; *Appl. Phys. Lett*, 96, 123114(2010).
- [8] M. Bender, N. Katsarakis, E. Gagaoudakis, E. Hourdakis, E. Douloufakis, V. Cimalla and G. Kiriakidis,; *J. Appl. Phys*, 90, 5382 (2001).
- [9] K.M. Sandeep, S. Bhat and S.M. Dharmaprakash,; *Mater. Sci. Semicond. Process*, 56, 265 (2016).
- [10] N.Z. Razali, A.H. Abdullaha and M.J. Haron,; *Adv. Mater. Res*, 364, 402 (2012).
- [11] P. Deepa, V. Sivaranjani and P. Philominathan,; *Int. J. Thin. Fil. Sci. Tec*, 4, 133 (2015).
- [12] S. J. Wen, G. Couturier, G. Campet, J. Portier and J. Claveri,; *Phys. Stat. Sol. (a)*, 130, 407 (1992).
- [13] M. Singh, V.N. Singh and B.R. Mehta,; *J. Nanosci. Nanotechnol*, 8, 3889 (2008).
- [14] S. Kaleemulla, N.M. Rao, N.S. Krishna, M. Kuppan and M. R. Begam and M. Shobana,; *J. Nano-Electron. Phys*, 5, 04048 (2013).
- [15] P. Deepa, V. Sivaranjani and P. Philominathan,; *Int. J. Chem Tech Res*, 6, 1939 (2014).
- [16] N.S. Krishna, S. Kaleemulla, G. Amarendra, N.M. Rao, C. Krishnamoorthi, M.R. Begam, I. Omkaram and D.S. Reddy,; *J. Supercond. Novel Magn*, 28(7) 2089 (2015).
- [17] P.K.S Rao, S. Krishnan, M. Pattabi and G. Sanjeev,; *Int. J. ChemTech Res*, 7(3), 1377 (2014-2015).
- [18] S. Kilarikaje, V. Manjunatha, S. Raghu, M.V.N.A. Prasad and H. Devendrappa,; *J. Phys. D: Appl. Phys.* 44, 105403 (2011).
- [19] G.M. Lohar, H.D. Dhaygude, B.P. Relekar, M.C. Rath and V.J. Fulari,; *Ionics*, 22(8), 1451 (2016).
- [20] D. Sarkar, G. Sanjeev and M.G. Mahesha,; *Radiat. Phys. Chem*, 98, 64 (2014).
- [21] J.J. Hren, J.I. Goldstein and D.C. Joy, *Introduction to Analytical electron microscopy*, 1st ed. (New York, NY: Springer Science+Business Media ,1979), pp.438-440.
- [22] D.V. Myroniuk, A.I. Ievtushenko, G.V. Lashkarev, V.T. Maslyuk, I.I. Timofeeva, V.A. Baturin, O.Y. Karpenko, V.M. Kuznetsov and M.V. Dranchuk,; *Semicond. Phys., Quantum Electron. Optoelectron*, 18, 286 (2015).
- [23] K.H.L. Zhang, A. Walsh, C.R.A. Catlow, V.K. Lazarov and R.G. Egdell,; *Nano Lett*, 10 (9), 3740 (2010).
- [24] S.S. Dhasade, S. Patil, B.B. Kale, S.H. Han, M.C. Rath and V.J. Fulari,; *Mater. Lett*, 93, 316 (2013).
- [25] U. Ozgur, A. Teke, C. Liu, S.J. Cho, H. Morkoc, and H.O. Everitt,; *Appl. Phys. Lett*, 84, 3223 (2004).
- [26] R.R. Krishnan, K.G. Gopchandran, V.P.M. Pillai, V. Ganesan and V. Sathe,; *Appl. Surf. Sci*, 255, 7126 (2009).
- [27] C. Agashe, M.G. Takwale, B.R. Marathe and V.G. Bhide,; *Sol. Energy Mater.*, 17, 99 (1988).
- [28] H. Faiz, K. Siraj, M. F. Khan, M. Irshad, S. Majeed, M. S. Rafique and S. Naseem,; *J. Mater. Sci.: Mater. Electron*, 27, 8197 (2016).

- [29] B.D. Cullity, *Elements of X-ray Diffraction*, (Massachusetts, Addison-Wesley Publishing company, Inc.,1956), pp.99.
- [30] R. Sathyamoorthy, S. Chandramohan, P. Sudhagar, D. Kanjilal, D. Kabiraj, K. Asokan and K. P. Vijayakumar, *J Mater Sci*, 42, 6982 (2007).
- [31] S. Chandramohan, R. Sathyamoorthy, P. Sudhagar, D. Kanjilal, D. Kabiraj and K. Asokan, *Nucl. Instrum. Methods Phys. Res., B*, 254, 236(2007).
- [32] R. Koch, *J. Phys. Condensed Matter*, 6, 9519 (1994).
- [33] N. Illyaskutty, S. Sreedhar, H. Kohler, R. Philip, V. Rajan, V.P.M. Pillai, *J. Phys. Chem. C*, 117, 7818 (2013).
- [34] R. Kayestha, Sumati and K. Hajela, *Fed. Eur. Biochem. Soc.*, 368, 285 (1995).
- [35] A. Singhal, S.N. Achary, J. Manjanna, O.D. Jayakumar, R.M. Kadam and A.K. Tyagi, *J. Phys. Chem. C*, 113, 3600 (2009).
- [36] S. Kumar, K. Asokan, R.K. Singh, S. Chatterjee, D. Kanjilal and A.K. Ghosh, *RSC Adv.*, 4, 62123 (2014).
- [37] J. Vetelino and A. Reghu, *Introduction to Sensors*, (Suite, CRC Press, Taylor and Francis Group, 2011), pp.35.
- [38] G. Korotcenkov, *Handbook of Gas sensor materials*, (USA, Springer Science and Business Media, 2013), pp.89.
- [39] L.S. Miller, J.B. Mullin, *Electronic Materials: from Silicon to Organics*, (New York, Springer Science and Business Media, 1991), pp.502.
- [40] Z. Ma and S. Dai, *Heterogeneous Gold Catalysts and Catalysis*, (UK, The Royal Society of Chemistry, 2014), pp.490.
- [41] M.V.G.-Pirovano, A. Hofmann and J. Sauer, *Surf. Sci. Rep*, 62, 219 (2007).
- [42] N.-E. Sung, H.-K. Lee, K.H. Chae, J.P. Singh and I.-J. Lee, *J. Appl. Phys*, 122, 085304 (2017).
- [43] D. Tiwari and Steve Dunn, *J. Eur. Ceram. Soc*, 29, 2799 (2009).
- [44] Z. Yin, Z. Hu, H. Ye, F. Teng, C. Yang and A. Tang, *Applied Surface Science*, 307, 489 (2014).
- [45] S. Luo, W. Zhou, Z. Zhang, J. Shen, L. Liu, W. Ma, X. Zhao, D. Liu, L. Song, Y. Xiang, J. Zhou, S. Xie, and W. Chu, *Appl. Phys. Lett.*, 89, 093112 (2006).
- [46] V. Lulin, I. Zharsky and P. Zhukowski, *Acta Phys. Pol. A*, 123, 837 (2013).
- [47] G. Schon, *Surf. Sci*, 35, 96 (1973).
- [48] O. M. Berengue, A. D. Rodrigues, C. J. Dalmaschio, A.J.C. Lanfredi, E.R. Leite and A.J. Chiquito, *J. Phys. D: Appl. Phys*, 43, 045401 (2010).
- [49] L. Guo, X. Shen, G. Zhu and K. Chen, *Sens. Actuators B*, 155, 752 (2011).
- [50] R.L. Frost, J. Yang and W.N. Martens, *J. Therm. Anal. Calorim*, 100(1), 109 (2010).
- [51] R.R. Krishnan, R.S. Sreedharan, S.K. Sudheer, C. Sudarsanakumar, V. Ganesan, P. Srinivasan, V.P.M. Pillai, *Mater. Sci. Semicond. Process*, 37, 112 (2015).
- [52] B.G. Domene, H.M. Ortiz, O. Gomis, J.A. Sans, F. J. Manjón, A. Munoz, P.R. Hernandez, S.N. Achary, D. Errandonea, D. M. Garcia, A.H. Romero, A. Singhal and A.K. Tyagi, *J. Appl. Phys*, 112, 123511 (2012).

- [53] J. Gan, X. Lu, J. Wu, S. Xie, T. Zhai, M. Yu, Z. Zhang, Y. Mao, S.C.I. Wang, Y. Shen and Y. Tong, : *Sci. Rep*, 3 : 1021,1 (2013).
- [54] S. Elouali, L.G. Bloor, R. Binions, I.P. Parkin, C.J. Carmalt and J.A. Darr, : *Langmuir*, 28, 1879 (2012).
- [55] Q. Williams, R.J. Hemley, M.B. Kruger and R. Jeanloz, : *J. Geophys. Res*, 98 (B12), 22157 (1993).
- [56] J.I. Pankove, *Optical Processes in Semiconductors*, (New York, Dover Publications, Inc, 1971), pp.35.